



# The Influence of Various Hybrid Welding Parameters on Bead Geometry

*Arc power and transfer mode greatly affect bead width, penetration, and reinforcement*

BY M. EL RAYES, C. WALZ, AND G. SEPOLD

**ABSTRACT.** A series of hybrid welding (gas metal arc welding-CO<sub>2</sub> laser beam welding) experiments was conducted in which the two energy sources were coupled in one process zone on the surface of a 316L austenitic stainless steel workpiece. Arc and laser power were varied in order to study their influence on various bead dimensions. Arc power and, consequently, the mode of metal transfer have a great influence on bead width *W*, arc and laser penetration *M* and *L*, and bead reinforcement *R*. Increasing arc power increases *W* and *L*, whereas it reduces *M* and *R*. Laser power and hence the laser-induced metal vapor significantly influences the features of the metal transfer mode in the arc process. Higher laser powers prolong the arc burning time  $T_a$  at the expense of the short circuit frequency  $N_{sc}$ , which assists in increasing *M* and *L*. At constant laser power, the contribution of the *M* solely into the total penetration *M*+*L* is always bigger than that of the *L*.

## Introduction

The combination of laser beam welding (LBW) and conventional gas metal arc welding (GMAW) processes, called hybrid (e.g., Refs. 1–3) or arc-augmented laser welding (e.g., Refs. 5–7), has been investigated and in progress during the last two decades. The potential for this combination is to increase the weld bead penetration, width, and welding speed, which is difficult to realize with either laser or arc process by their own. Combining the two processes results in a new one with its inherent features and characteristics, hence widening the areas of its application and increasing its capabilities, once the mutual

interaction between the two energy sources is optimized. The arc welding process, characterized by relatively lower power density and wider process zone, gives a wide bead, thus enhancing the joint's root bridging ability and enlarging the manufacturing tolerances for joint preparation. Simultaneously, the laser beam process, characterized by higher localized power density, leads to a deeper penetration. Thus in hybrid GMA-laser beam welding, a wide and deep bead is achieved at higher welding speeds when compared with the GMAW process by its own (Ref. 8). This accordingly leads to less heat input per unit length, less thermal distortion, and therefore, less residual stresses, narrower heat-affected zone (HAZ), and more important, increased productivity.

## Hybrid Welding Principles

Figure 1 shows a sketch of the hybrid welding process (Ref. 10). In hybrid welding, a gas or solid-state laser (e.g., CO<sub>2</sub> or Nd:YAG) is combined with an arc welding process (e.g., GMAW, GTAW, or PAW) (Refs. 2, 3, 9). Both processes supply energy to the work surface. The focused laser beam impinges the workpiece surface converting its energy into heat. This causes vaporization of the workpiece material and formation of a deep vapor-filled capillary, i.e. keyhole, which is stabilized by the pres-

sure of the metal vapor being generated. This metal vapor is capable of becoming hotter and forms a laser-induced plasma (Refs. 2, 9) that emerges from the keyhole causing attenuation of the laser beam above the work surface. This is called plasma-shielding effect, and its extent depends upon the gas type, electron density, and laser wavelength (Ref. 9). In order to reduce the plasma effect, a process gas with high ionization potential, normally helium, is used. In addition, the power of the arc welding process introduces more energy to the zone of laser beam impingement causing the process gas to be ionized, thus enhancing arc stability.

Principally, LBW can be combined or coupled with the arc welding process as shown in Fig. 2 (Ref. 3). When combined, they act separately with respect to time and zone and no mutual interaction takes place. This technique is used in single-side welding of thick-walled components such as pipeline fabrication and in shipbuilding, in which the laser beam bridges the root followed by the arc process (GMAW) (Ref. 3). When the two processes are coupled as one process, the laser beam and the arc process interact simultaneously in one zone and mutually influence one another. Such process coupling is referred to by the term "Hybrid Welding Process."

The gas type used in such process has a significant influence upon the plasma formation and arc stability in the hybrid process. Helium has a higher ionization potential than argon and therefore produces less dense plasma, hence, its use is beneficial in laser welding at low speeds and higher powers as there will be less attenuation of the beam. Conversely, argon produces denser plasma, which hinders deeper beam penetration but is advantageous for arc stability (Refs. 2, 6). It can be concluded that the effects of gas components in hybrid welding are contradictory in their function (Ref. 8), which requires

## KEY WORDS

Bead Geometry  
 Gas Metal Arc  
 Hybrid Welding  
 Laser  
 Short Circuit  
 Stainless Steel

*M. EL RAYES is with Production Engineering Department, Faculty of Engineering, Alexandria, Egypt. C. WALZ and G. SEPOLD are with Bremen Institute for Applied Beam Technology BIAS, Bremen, Germany.*

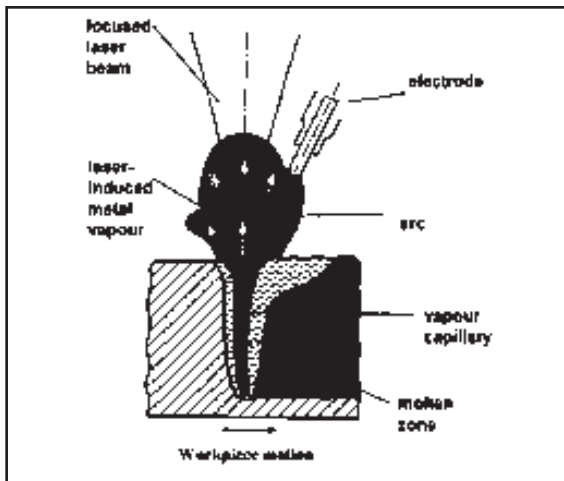


Fig. 1 — Hybrid welding process principles (Ref. 10)

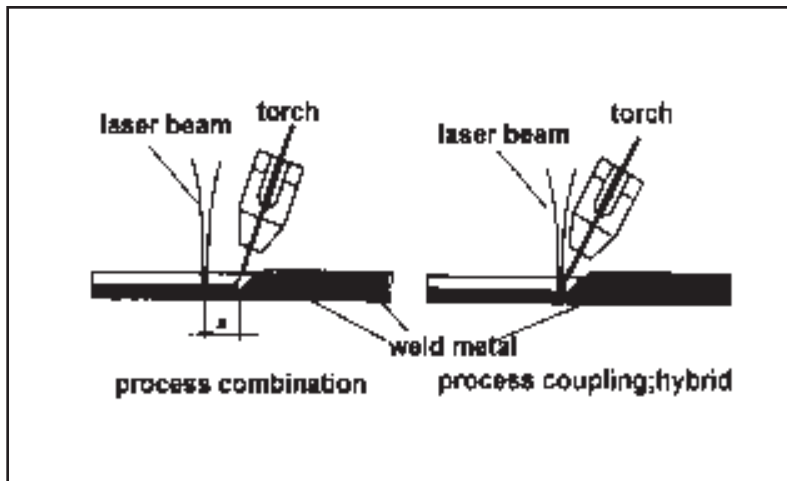


Fig. 2 — Process combination (they are separated by distance  $a$ ) and process coupling in hybrid welding (Ref. 3).

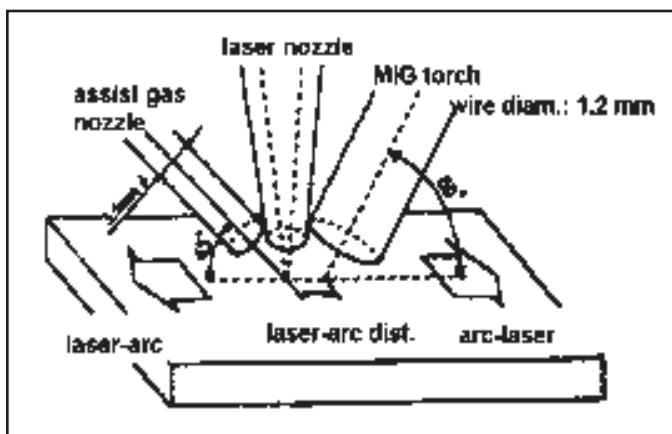


Fig. 3 — Arc-laser or laser-arc arrangement with respect to welding direction (Ref. 8).

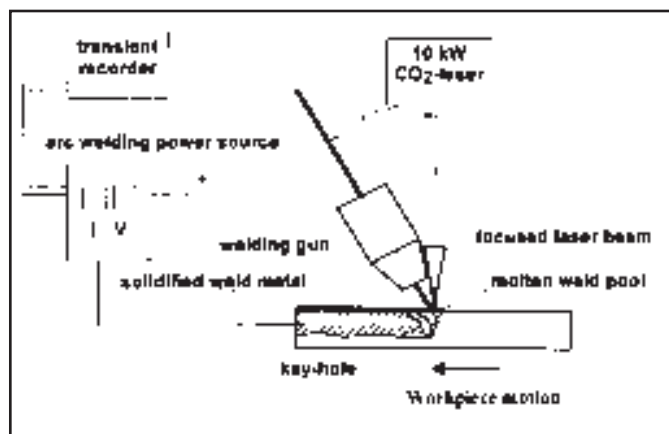


Fig. 4 — Schematic drawing of experimental setup.

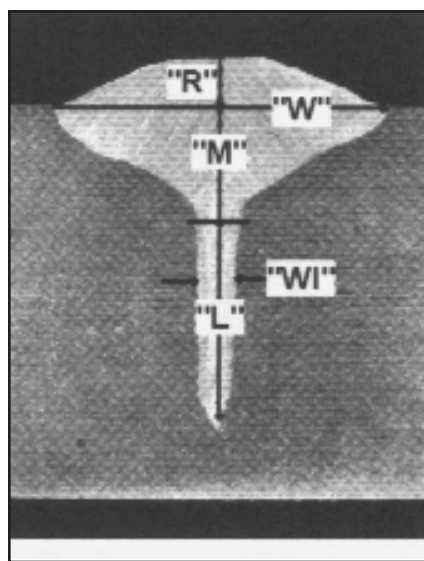


Fig. 5 — Nomenclature of weld bead dimensions (5 $\times$ ).

an appropriate gas composition that optimally reduces the plasma shielding effect and also enhances arc stability. In hybrid welding, there are numerous parameters that should be adjusted. They are classified (Refs. 2, 4) according to the parameters involved in laser (e.g., type, focal length, etc.) and base metal (e.g., type, joint design, etc.).

### Influence of Hybrid Welding Process Parameters on Bead Shape

The distance between the arc and the laser beam (arc is leading) was found to influence the bead penetration. The smaller this distance gets, the deeper the penetration. This is because the laser beam impinges and penetrates the hot weld pool more readily than a solid surface, which occurs with longer distances. Varying this distance from 0 to 50 mm for deepest penetration yielded to an optimum value of 0

mm (Ref. 5) and 7 mm (Ref. 8), although the same laser type ( $\text{CO}_2$ ), arc process (GMAW), and welding direction (arc is leading) were used. This range is seen to be relatively wide and needs to be studied further. The location of the laser beam focal point with respect to the workpiece surface in conjunction to welding current was also found to affect the bead penetration. At constant laser power and welding speed, the higher the current, the deeper the focal point should be under the work surface in order to realize deepest penetration (Ref. 5). The reason is basically due to the current increase, which causes an increase in the size and depth of the weld pool. If the focal point of the laser beam is set initially at the work surface, it will be above the surface of the resultant weld pool and not give maximum penetration.

In addition, the arrangement of the two welding processes, laser-arc or arc-laser, in the welding direction (Fig. 3) has

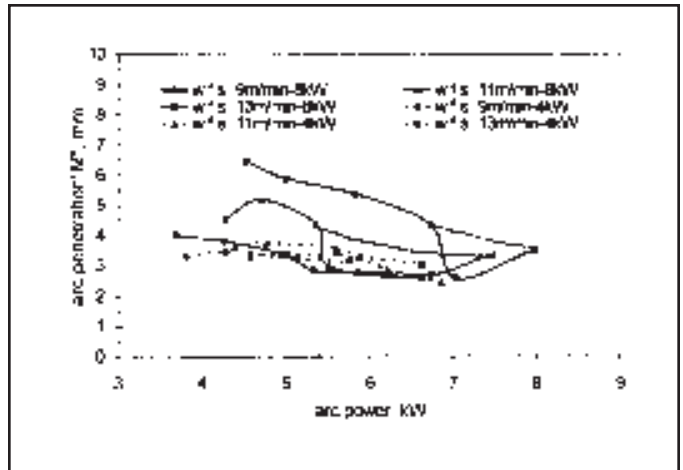
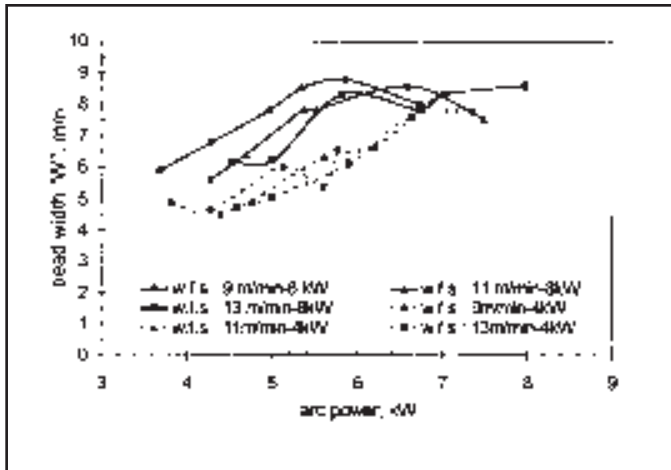


Fig. 6 — Relationship between arc power and bead width, *W*.

Fig. 7 — Relationship between arc power and arc penetration, *M*.

a significant importance in the hybrid process (Ref. 8). The former arrangement (the laser beam precedes the arc) was found to be superior regarding the bead appearance, because the assist gas flow does not affect the molten pool created by the arc. Whereas, in the later arrangement, the shape of the bead surface is disrupted by the assist gas blowing into the molten pool. Nevertheless, it was reported that arc-laser arrangement gives a more stable arc (Ref. 2).

The mutual influence between laser and arc energy sources differs in intensity and form depending upon the utilized parameters of each process (Ref. 11). Therefore, an important characteristic of hybrid welding is the ratio of power between the two energy sources, which determines if the laser or arc process is more dominant as to penetration depth and width. This depends upon the selected power for each process that in turn influences the bead shape (Ref. 12). It has been noted from the available literature that the dependence of the mutual interaction, between the laser and arc processes, upon the power ratio was not sufficiently clarified. This is probably due to the displacement created between the laser beam and arc column in the earlier work, thus demanding further investigations with zero displacement.

In spite of the increased number of variable parameters due to the process coupling, the large number of mutual interactions of individual factors and the lack of reference data, the present work is devoted to three main objectives. 1) Establish and ascertain basic relationships between the hybrid process main parameters (arc and laser power) and various bead dimensions. 2) Correlate these relationships with the possible interactions between the two processes. 3) Widen the

**Table 1 — Hybrid Welding Parameters Varied during Experiments**

| Laser Power, kW | Arc Power = Mean Welding Current × Mean Arc Voltage                         |    |    |    |  |    |    |    |  |    |    |    |    |    |    |
|-----------------|---|----|----|----|--|----|----|----|--|----|----|----|----|----|----|
|                 | wfs <sup>(a)</sup> = 9 m/min<br><i>I<sub>m</sub></i> <sup>(b)</sup> ~ 230 A |    |    |    | wfs = 11 m/min<br><i>I<sub>m</sub></i> ~ 260 A |    |    |    | wfs = 13 m/min<br><i>I<sub>m</sub></i> ~ 290 A |    |    |    |    |    |    |
|                 | Set Arc Voltage   |    |    |    | Set Arc Voltage                                |    |    |    | Set Arc Voltage                                |    |    |    |    |    |    |
| 4               | 19  | 21 | 24 | 26 | 28   | 19 | 21 | 24 | 26   | 28 | 19 | 21 | 24 | 26 | 28 |
| 6               | 19  | 21 | 24 | 26 | 28   | 19 | 21 | 24 | 26   | 28 | 19 | 21 | 24 | 26 | 28 |
| 8               | 19  | 21 | 24 | 26 | 28   | 19 | 21 | 24 | 26   | 28 | 19 | 21 | 24 | 26 | 28 |
| 9               | 19  | 21 | 24 | 26 | 28   | 19 | 21 | 24 | 26   | 28 | 19 | 21 | 24 | 26 | 28 |

(a) wfs = wire feed speed.  
(b) *I<sub>m</sub>* = mean welding current.

scope of the hybrid process with respect to base material type and thickness; through exploiting the process advantages (e.g., high welding speeds, deep penetration, gap bridging ability, less distortion, etc.) on thick base metals. The base material type chosen is austenitic stainless steel, which is often used in pipeline, tank, and offshore structure fabrication.

## Experimental Work

### Energy Sources and Materials

In this work, a 10-kW, CO<sub>2</sub> laser was used. The laser beam was focused with a parabolic reflective 90-deg optics via an O<sub>2</sub>-free copper mirror of a 300-mm focal length. The spot diameter of the focused beam was 0.8 mm. In conjunction, a multifunctional GMAW power source was used, which supplies 400 A/34 V at 100% duty cycle. The base material used was commercial austenitic stainless steel plates (DIN: 1.4404, AISI: 316L), which were sawed into 220 × 100 × 10 mm strips. An austenitic stainless steel filler metal

(DIN: 1.4302, AWS: ER308) was used having 1.2-mm diameter and direct-current, electrode-positive (DCEP) polarity. A standard mixture of shielding gas (75%He-23%Ar-2%O<sub>2</sub>) flowing at 30 L/min was used.

### Experimental Setup

Figure 4 shows the experimental setup of the present work. The GMAW gun position was fixed during the experiments, having an inclination of 30 deg from the vertical laser beam, and an electrode extension of 15 mm. The specimen mounted on a carriage was moved at a speed of 30 mm/s, which was kept constant during the experiments. Welding current and arc voltage traces were recorded via a transient recorder. After welding, macrosections of the weld beads were ground, polished, and etched according to the standard procedures. All these sections were cut midway from the welded specimen. The bead dimensions corresponding to each welding parameter were measured using a stereo microscope with 0.1 mm sensitivity.

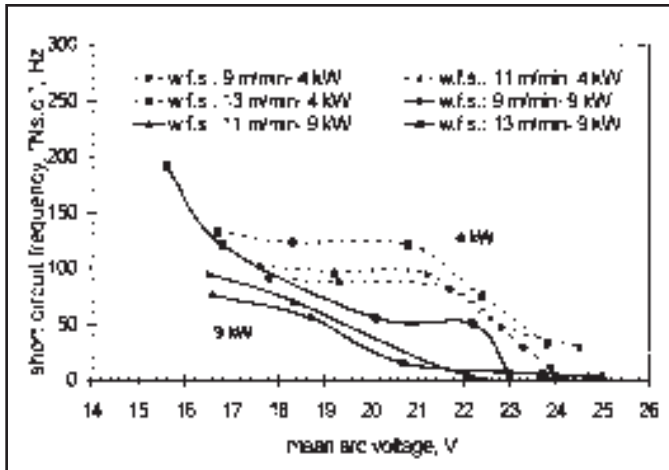


Fig. 8 — Relationship between short-circuit frequency,  $N_{sc}$  and mean arc voltage.

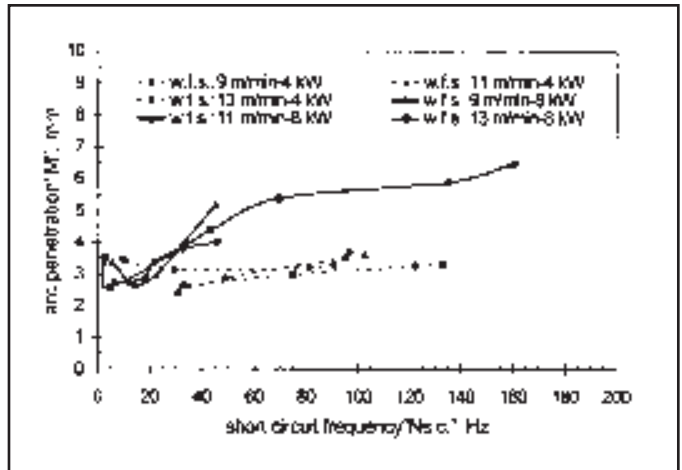


Fig. 10 — The dependence of arc penetration  $M$  upon the short-circuiting frequency  $N_{sc}$ .

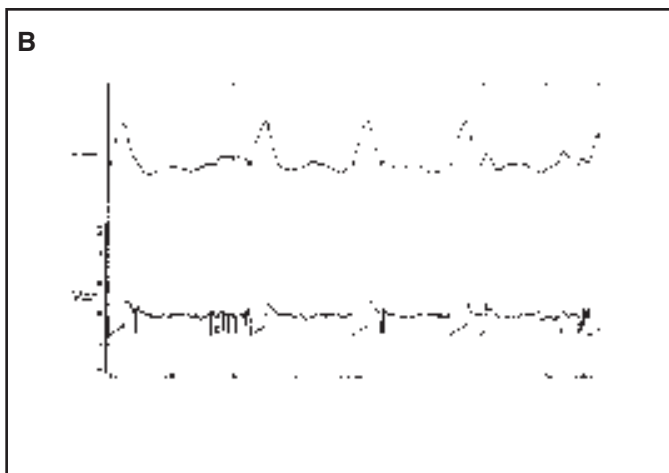
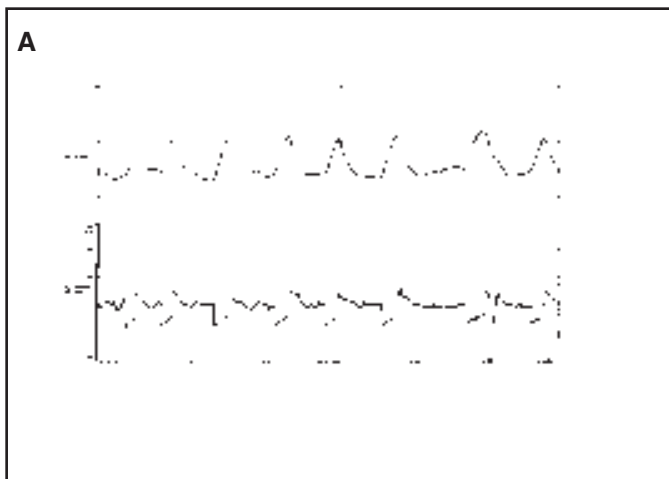


Fig. 9 — Current (upper)–voltage (lower) signals recorded with time (ms) during hybrid welding at laser power of: A — 4 kW; B — 9 kW.

### Experimental Parameters

Table 1 presents the welding parameters that were varied during experiments. For each combination of laser power, wire feed speed, and arc voltage, a power ratio

workpiece surface to the top of the bead.  $M$  is arc penetration measured from the work surface to the extent of the weld cast structure.  $L$  is laser beam penetration calculated as the protruding penetration be-

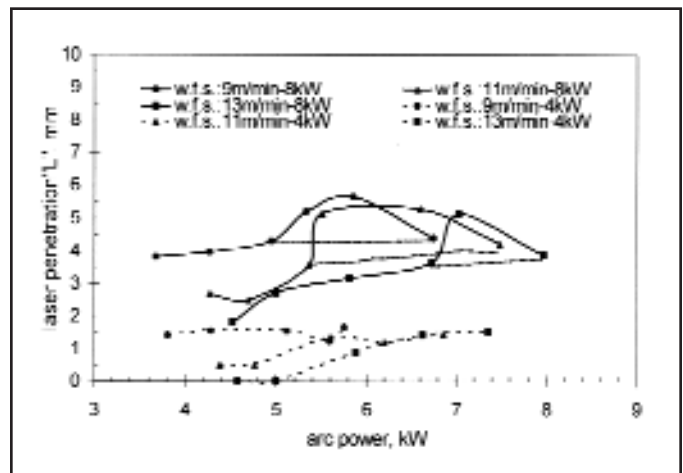


Fig. 11 — Relationship between arc power and laser penetration  $L$ .

was calculated by dividing arc power by laser power.

### Bead Dimensions Nomenclature

In this study the bead geometry was divided into five dimensions, as shown in Fig. 5.  $W$  is bead width, measured between the two weld interfaces intersecting with the workpiece surface.  $R$  is bead reinforcement, measured from the workpiece surface to the top of the bead.  $M$  is arc penetration measured from the work surface to the extent of the weld cast structure.  $L$  is laser beam penetration calculated as the protruding penetration be-

yond  $M$ , measured from the end of  $M$ , until the end of penetration.  $M+L$  is total penetration as the sum of  $M$  and  $L$ .  $W_L$  is laser beam penetration width.

### Results and Discussion

#### Effect of Arc Power on Bead Geometry

At constant wire feed speed (called wfs hereafter) and laser power, increasing arc power increases the bead width  $W$  until a maximum is reached. Beyond this maximum value,  $W$  decreases with wfs of 9 and 11 m/min, or stays unchanged with 13 m/min — Fig. 6. As presented in Table 1, the arc power was mainly increased by increasing arc voltage at a constant wfs, thus creating longer arc lengths, which is followed by increasing the arc diameter and consequently widening the wetting zone on the workpiece surface. This causes a wider bead until a maximum width is reached. With still higher arc power, the wetting zone is further widened, but the

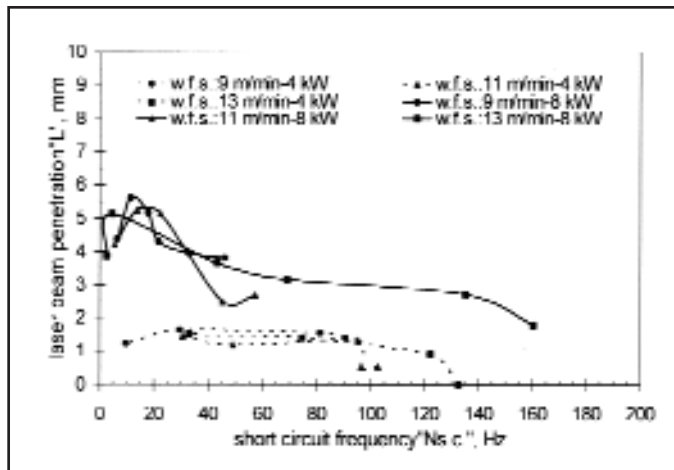


Fig. 12 — The dependence of laser penetration  $L$  upon the short-circuit frequency  $N_{sc}$ .

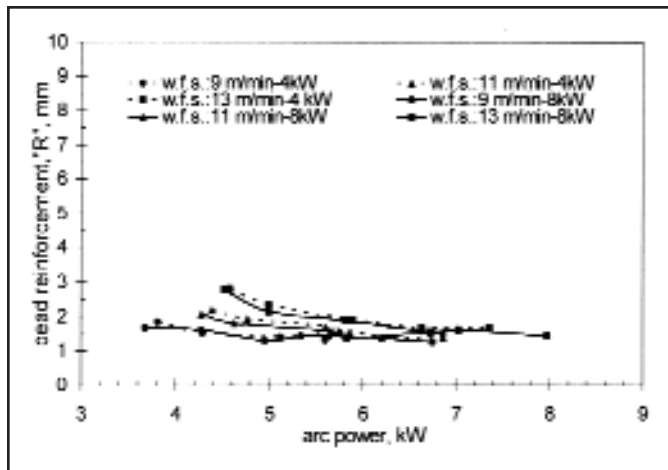


Fig. 13 — Relationship between arc power and bead reinforcement  $R$ .

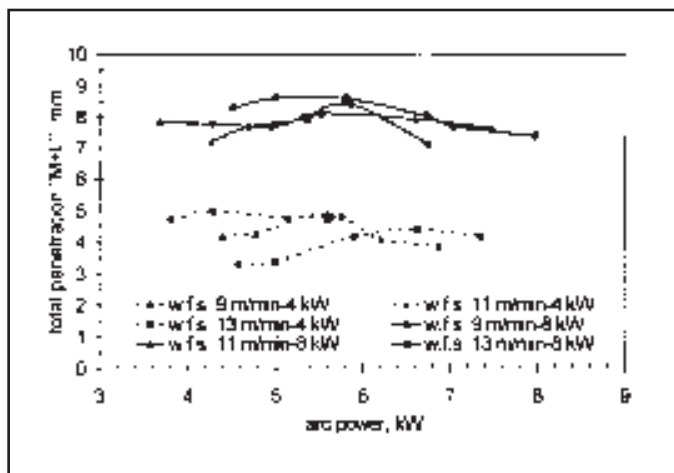


Fig. 14 — Relationship between arc power and total penetration  $M+L$ .

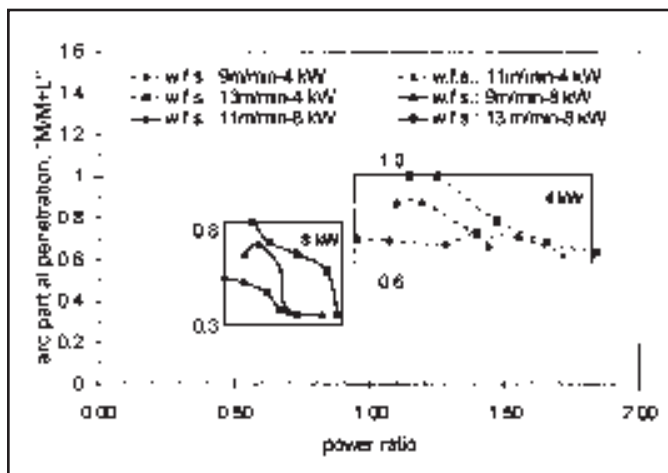


Fig. 15 — Relationship between power ratio and arc partial penetration  $M/M+L$ .

metal deposited has become insufficient with wfs of 9 and 11 m/min or just enough, with 13 m/min to fill that zone. Figure 6 also shows that at a constant laser and arc power, increasing the wfs reduces the  $W$ . Figure 7 correlates this result with arc penetration  $M$ . At constant laser and arc power, increasing the wfs deepens the  $M$ . In the same figure, increasing the arc power reduces the  $M$  penetration. The mode of metal transfer is an explanation for the reduction of  $M$ . At low arc power, i.e., low current and voltage, a short-circuiting transfer mode with its accompanying strong weld pool dynamics occurs causing a relatively deeper  $M$ . On the other hand, with increased arc power, a spray transfer mode is reached with calmer weld pool resulting in a shallower  $M$ . In order to clarify the above-mentioned explanation, the relationship between arc voltage and the short-circuit frequency  $N_{sc}$  is presented in Fig. 8. Increasing arc voltage is accompanied by

a gradual change from short-circuiting transfer toward a spray transfer mode. In addition, the  $N_{sc}$  occurring with the 4-kW laser power is relatively higher than that with 9 kW. The reason is perhaps due to the greater amount of metal vapor produced by 9 kW than that by 4 kW. This metal vapor enhances current conduction and also reduces the arc voltage, based on the fact that metal vapor possesses relatively lower ionization potential than a shielding gas does (Ref. 13). As a consequence, the arc burning time, defined as the time elapsed during which the arc burns between two consecutive short circuits, is prolonged at the expense of the  $N_{sc}$  for a constant recording time. Figure 9 shows two current-voltage traces occurring at 4- and 9-kW laser power, respectively, using the same welding parameters. Longer arcing times are noticed with the 9-kW signal than with 4 kW.

Furthermore, Fig. 10 shows the dependence of arc penetration  $M$  upon the  $N_{sc}$ .

Generally, as the  $N_{sc}$  increases,  $M$  also increases. This result is clearer when higher laser powers (8 kW) are used, where the variation of  $M$  is more pronounced than that with 4 kW. This is probably due to the higher heat input per unit length and consequently higher heat content of the weld pool. This causes the weld pool to be more dynamic leading to a deeper  $M$  especially within the short-circuiting mode.

The laser beam penetration  $L$  generally increases with higher arc power, as seen in Fig. 11. The reason can also be attributed to the mode of metal transfer occurring with the arc process. As already known, the end of a short-circuiting period, i.e. the moment of arc reignition, is characterized by an explosion of the molten bridge that had connected the molten electrode wire tip with the weld pool and also by a sudden and intensive current flow through the arc. These two incidents have a double effect. First, they disturb the shielding gas flow, which the

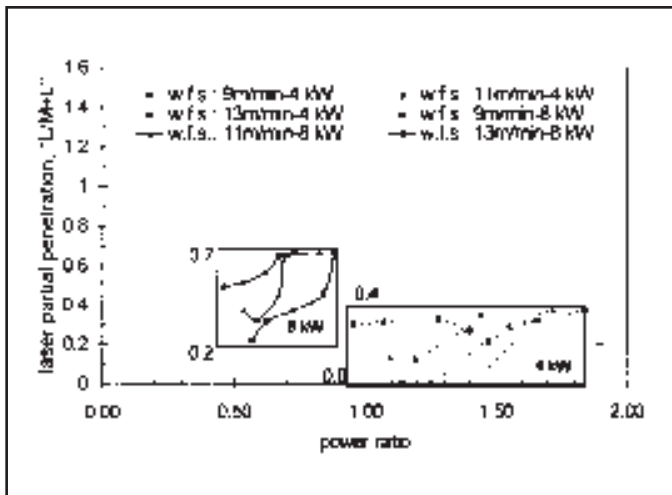


Fig. 16 — Relationship between power ratio and laser partial penetration,  $L/(M+L)$ .

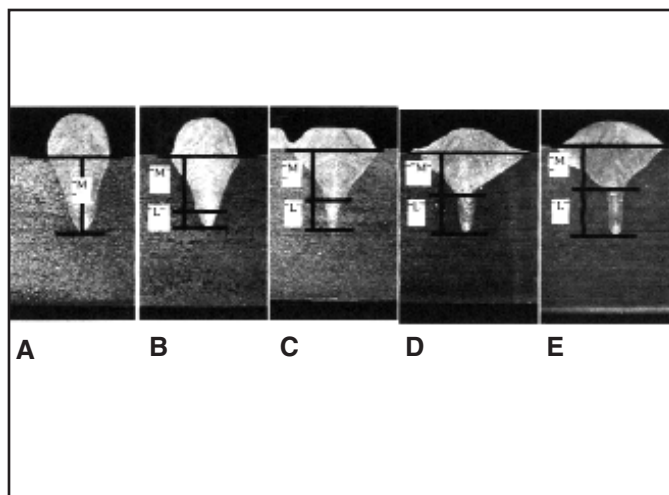


Fig. 17 — General influence of short-circuiting frequency  $N_{sc}$  on bead geometry at constant laser power (6 kW) and w.f.s (13 m/min). A — 173 Hz; B — 106 Hz; C — 89 Hz; D — 45 Hz; E — 19 Hz.

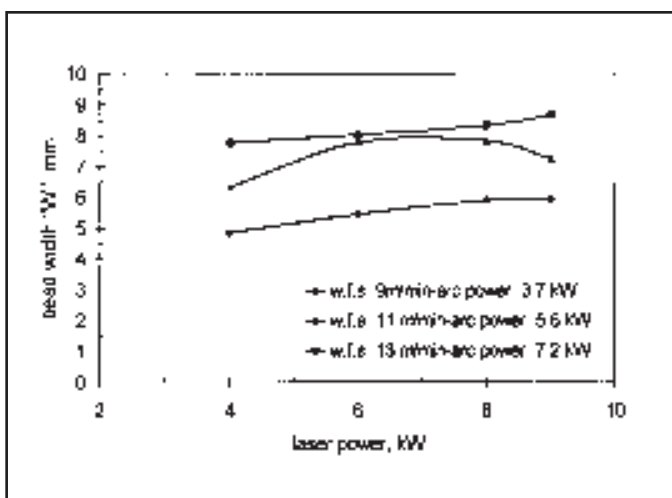


Fig. 18 — Relationship between laser power and bead width  $W$ .

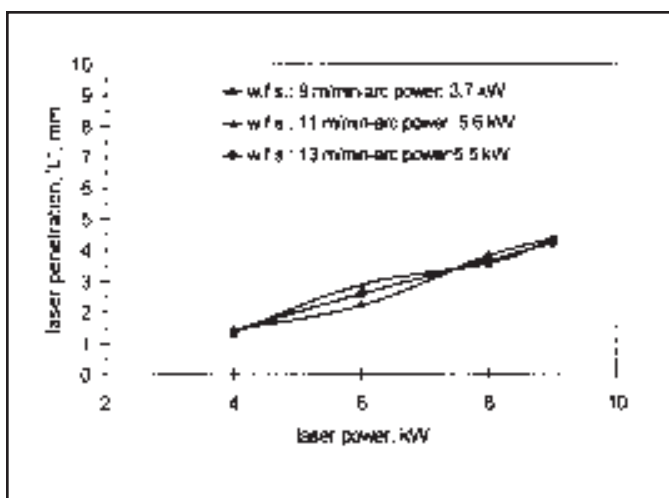


Fig. 19 — Relationship between laser power and laser beam penetration  $L$ .

laser beam requires to realize its deep penetration. Second, they depress the weld pool surface leading to a wavy motion, thus changing the interaction with the laser beam at a frequency similar to that of the short circuits. Figure 12 shows the dependence of  $L$  upon the  $N_{sc}$ . At low  $N_{sc}$ , i.e., almost spray transfer mode,  $L$  penetration is maximum, where the molten pool is less dynamic, beyond which it gradually declines with higher  $N_{sc}$ .

It is obvious that with 8-kW laser power,  $M$  and  $L$  were subjected to abrupt change when plotted against arc power — Figs. 7 and 11. For both dimensions, these changes occurred at the same arc powers of 5.3, 5.5, and 7.0 kW corresponding to w.f.s of 9, 11, and 13 m/min, respectively. These values of arc power are specific and

are only valid for 8-kW laser power, because at 4 kW, no abrupt changes took place as seen in the same figures. By omitting the abrupt fall or rise of  $M$  or  $L$ , and extrapolating the rest of the curves, dotted lines in Figs. 7 and 11, they take smooth trends without further abrupt changes.

Figures 10 and 12 show, at their extreme left in a narrow range between 5~20 Hz, similar changes in  $M$  and  $L$  when plotted against the  $N_{sc}$ . In this range, the transfer is described as spray with occasional short circuits. This possibly indicates that the shielding medium occurring with 8-kW laser power has the highest ionization potential compared to media occurring with 4-, 6-, and 9-kW laser powers. High-ionization potential gas mixture possesses relatively low current conduction,

thus limiting  $M$ , and also low-density plasma, thus enhancing  $L$ . In this respect, further investigations covering a wider range of parameters with closer process monitoring is presently conducted.

The relationship between arc power and the bead reinforcement  $R$  is presented in Fig. 13. The higher the arc power is, i.e., going toward the spray transfer mode, the more the reduction in  $R$  occurs, where the bead becomes flatter and also wider as shown in Fig. 6.

Figure 14 shows that with increasing arc power the total penetration  $M+L$  is slightly reduced, whereas increasing laser power markedly increases it. Worth noting that in spite of the sudden changes of  $M$  and  $L$  when varying arc power (Figs. 7 and 11), the  $M+L$  showed a continuous trend, i.e. with-

out abrupt changes. This means that M compensates L or vice versa. Therefore, it is important to distinguish between the contribution of M solely and similarly L with respect to M+L. For this reason the terms arc partial penetration and laser partial penetration were introduced. The former term is expressed by dividing M by M+L and the later L by M+L. Figures 15 and 16 show these terms in enclosed windows when plotted against the power ratio at different wfs and laser powers. At constant laser power, e.g., 8 or 4 kW, increasing power ratio reduces the M/M+L. This is because of the increased arc power leading to spray transfer, as mentioned in Fig. 7, hence reducing M with respect to M+L. The same reason also causes the L to increase with increasing power ratio as in Fig. 16. The comparison between the locations of the windows indicate that with 4-kW laser power, the M value contributes between 60~100% in the M+L (100% means no protruding laser penetration), whereas L contributes between 0.0~40%. With 8 kW, the contribution of M and L became similar, however, the M share (30~80%) is still higher than that of L (20~70%). Therefore, it could be stated that at low laser powers M dominates the M+L, whereas, at higher ones, M and L have similar shares.

Within the entire range of arc power investigated, it has almost no effect on the laser penetration width Wl, whereas the laser power is slightly more influential. Higher laser powers result in wider Wl, because of the greater melting and evaporation capability. According to the hitherto discussion, the  $N_{sc}$  has generally a great influence on bead geometry. Figure 17 shows this influence on beads welded at different  $N_{sc}$ , at constant laser power (6 kW) and wfs (13 m/min).

### Effect of Laser Power on Bead Geometry

Although the effect of laser power is mentioned in the previous section, the results of the investigated full range laser power will be presented. Figure 18 shows the effect of laser power on W at three different arc powers. Increasing the laser power increases the amount of molten metal causing the bead to become wider. At constant laser power, increasing arc power increases the bead width. This result is in good agreement with that mentioned in the previous section — Fig. 6.

The effect of increasing laser power on L, R, and Wl has been studied. Increasing laser power significantly affects the penetration L, as seen in Fig. 19, whereas it has almost no influence upon R and Wl. At constant laser power, the arc power more or less has a negligible influence upon L, R, and Wl.

### Conclusions

According to the chosen set of welding parameters in hybrid GMA-CO<sub>2</sub> laser beam welding and referring to the aforementioned results and discussions, the conclusions are as follows:

- 1) A relationship exists between arc power and W, M, and R. Increasing arc power increases W and reduces both M and R.
- 2) The mode of metal transfer occurring with the arc process plays an important role in determining the extent of not only M but also L.
- 3) Laser power and consequently the amount of laser-induced metal vapor influence the features of metal transfer in the arc process. It prolongs the arc burning  $T_a$  time on the expense of the short-circuit frequency  $N_{sc}$ .
- 4) Although the share of M in M+L is more dominant than the L share, increasing the laser power increases the L share in the M+L.
- 5) Increasing laser power increases W and L, whereas, it has a negligible influence upon R and Wl.

### References

1. Dilthey, U., Keller, H., and Ghandahari, A. 1999. Laser beam welding with filler metal. *Steel Research* 70(4/5): 198–202.
2. Dilthey, U., Lueder, F., and Wieschemann, A. 1999. Expanded capabilities in welding of aluminium alloys with laser-MIG hybrid process. *Aluminium* 75(1/2): 64–75.
3. Dilthey, U., and Wieschemann, A. 1999. Prospects by combining and coupling laser beam and arc welding processes, IIV Doc. XII-1565-99, p. 1–16.
4. Dilthey, U., Lueder, F., and Wieschemann, A. Technical and economical advantages by synergies in laser hybrid welding. Technical Report, ISF, Welding Institute, Aachen University, Germany.
5. Matsuda, J., Utsumi, A., Hamasaki, M., and Nagata, S. 1988. TIG or MIG arc augmented laser welding of thick mild steel plate. *Joining and Materials*, pp. 31–34.
6. Alexander, J., and Steen, W. M. Arc augmented laser welding-process variables, structure and properties. *The Joining of Metals: Practice and Performance*, pp. 155–160.
7. Steen, W. M., and Eboo, M. 1979. Arc augmented laser welding. *Metal Construction*, pp. 332–335.
8. Abe, N., Agamo, Y., Tsukamoto, M., Makino, T., Hayashi, M., and Kurosawa, T. 1997. High speed welding of thick plates on laser-arc combination system. *JWRI* 26(1): 69–75.
9. Bayer, E., Imhoff, R., and Neuenhahn, J. 1994. A new welding technique and device for enhanced welding efficiency. *IBEC'94, Advanced Technology and Processes*, pp. 101–103.

10. Behler, K., Neuenhahn, J., Maier, C., Beersiek, J., Imhoff, R., and Bayer, E. 1995. Prozesstechnische Aspekte der Kombination des Laserstrahl und Lichtbogenschweißens. *Mechanik und Optik-Hochleistungslaser im Maschinenbau*, ISL, 25-27.04, pp. 33–47.
11. Dilthey, U., Brandenburg, A., and Wieschemann, A. 1999. Laser-beam-GMA-hybrid welding of steel and aluminium. *JOM-9 Proceedings*, pp. 66–70.
12. Maier, C., Reinhold, P., Maly, H., Behler, K., and Bayer, E. 1996. Aluminiumstrangpressprofile im Schienenfahrzeugbau, geschweisst mit dem Hybridverfahren: Nd:YAG-laser/MIG, DVS-Report, Band (176), Duesseldorf, *DVS Verlag*, p. 198–202.
13. Lancaster, J. F. 1985. *The Physics of Welding*, 2nd Edition, Pergamon Press.

**ARE YOU UP  
TO STANDARD?**  
[www.aws.org/catalogs](http://www.aws.org/catalogs)

**CLICK FOR  
CODE SECRETS**  
[www.aws.org/catalogs](http://www.aws.org/catalogs)

**HOTTEST WELDING  
BOOKS ON THE WEB**  
[www.aws.org/catalogs](http://www.aws.org/catalogs)

### Change of Address? Moving?

Make sure delivery of your *Welding Journal* is not interrupted. Contact the Membership Department with your new address information — (800) 443-9353, ext. 480; [jleon@aws.org](mailto:jleon@aws.org).